Available online at www.sciencedirect.com
ScienceDirect
Applied Catalysis B: Environmental 83 (2008) 56–62
APPLIED CATALYSIS B: ENVIRONMENTAL
www.elsevier.com/locate/apcatb

Visible-light-induced photocatalytic oxidation of carboxylic acids and aldehydes over N-doped TiO_2 loaded with Fe, Cu or Pt

Takeshi Morikawa [a,*], Takeshi Ohwaki [a], Ken-ichi Suzuki [a], Shinya Moribe [a], Shozo Tero-Kubota [b]

[a] *Toyota Central Research and Development Laboratories, Inc., Nagakute, Aichi 480-1192, Japan*
[b] *Institute of Multidisciplinary Research for Advanced Materials, Tohoku University, Katahira 2-1-1, Aobaku, Sendai 980-8577, Japan*

Received 24 September 2007; received in revised form 26 January 2008; accepted 29 January 2008
Available online 9 February 2008

Abstract

The rates of photocatalytic oxidation of gaseous formic acid, acetic acid, acetaldehyde and toluene over N-doped TiO_2 ($TiO_{2-x}N_x$) loaded with Fe, Cu or Pt were determined under visible light irradiation (>410 nm). It was found that the loading of Fe, Cu or Pt resulted in similar rates of enhancement of acetaldehyde oxidation, and that Cu and Pt gave the highest rates of acetic acid and toluene oxidation, respectively. It was also confirmed that the rate of formic acid photooxidation was enhanced by factors of 5 and 22 on loading of Fe and Pt, respectively. The extremely high rate enhancement of formic acid oxidation over Pt–$TiO_{2-x}N_x$ was found to be due to a combined effect of photocatalysis and thermal catalysis at room temperature facilitated by nanoscale (1–2 nm) Pt. These results indicate several important points as to enhancement of the activity of $TiO_{2-x}N_x$ modified with metallic species.

Keywords: Nitrogen; Doping; TiO_2; Platinum; Iron; Copper; Visible light; Acetaldehyde; Formic acid; Acetic acid

1. Introduction

TiO_2 shows excellent photocatalytic activity for the oxidative detoxification of organic pollutants [1–5]. However, the main issue to be taken into consideration is that TiO_2 photocatalysts can only be excited with UV light because of their wide band gap. To widen the area of their practical application to indoor use, it has been considered that photocatalysts which can be activated under visible light with high yields are indispensable. For this purpose, in recent years, much attention has been paid to the doping of TiO_2 with non-metallic or anionic species. In particular, doping with nitrogen [5–7], carbon [8], and sulfur [9,10] have been considered significant.

Nitrogen-doped TiO_2 ($TiO_{2-x}N_x$) appears promising because, for example, it can photodegrade formaldehyde at a 100 ppb flow under very low illuminance of 150 lx (corresponding to 44 $\mu W/cm^2$ within the range of 380–470 nm), which is as low as the average level in houses [11]. However, from the viewpoint of practical applications, a higher reaction rate is still required since the quantum efficiency of $TiO_{2-x}N_x$ under visible light is only 14% of that under UV light [7]. Furthermore, a serious problem regarding its oxidative power caused by N doping has been pointed out. The photogenerated holes in $TiO_{2-x}N_x$ fail to oxidize methanol, formic acid, and ethylene glycol in aqueous media owing to the potential of visible photons [12–14]. Among these organic substances, the oxidation of formic acid is the most significant because almost all organic pollutants have to undergo formic acid formation before being completely photooxidized to CO_2 and H_2O, as demonstrated on *in situ* DRIFT-GC analysis of the process of photooxidation of toluene [15]. Although it has been reported that formic acid can also be decomposed into CO_2 and H_2O in air [15], it was not clarified if the rate of photooxidation of formic acid is equivalent to those in the cases of acetaldehyde, toluene, etc. If it is lower, formic acid oxidation would be the rate-determining step for many photodegradation processes over $TiO_{2-x}N_x$ under visible light irradiation in the atmosphere. Since $TiO_{2-x}N_x$ is commercially produced at present [16], elucidating the rate-limiting step is crucial for its widespread indoor use. Furthermore, the priorities (or selectivity) of

* Corresponding author.
E-mail address: morikawa@mosk.tytlabs.co.jp (T. Morikawa).

0926-3373/$ – see front matter © 2008 Elsevier B.V. All rights reserved.
doi:10.1016/j.apcatb.2008.01.034

photodegradation in an actual multiple-gas environment will also be a controversial issue when photocatalysts are used in an environment with a high gas concentration or low illuminance [17]. In this regard, anyway, it is also indispensable to improve the rate of photodegradation of $TiO_{2-x}N_x$.

Loading co-catalysts onto the surface of oxide photocatalysts is one of the well-known methods for enhancing their activity. The loading of transition metal species onto TiO_2 has also been extensively studied in both gas–solid and liquid–solid regimes since they are believed to improve the photocatalytic activity due to enhancement of the adsorption of substances and separation of photogenerated electron–hole pairs [18–26].

Accordingly, the loading of metallic species onto the surface of $TiO_{2-x}N_x$ is considered to be the most realistic method in the context of enhancing the photocatalytic activity under visible light, taking into consideration the industrial production cost. However, reports on loading onto $TiO_{2-x}N_x$ have been few. Among them, it was recently reported that the loading of Cu ions (Cu^{1+} or hydrated form) or Pt improved the rate of photooxidation of acetaldehyde over visible-illuminated $TiO_{2-x}N_x$, but not that of Ni, Zn or La [27]. In particular, Cu^{1+} loaded $TiO_{2-x}N_x$ can photooxidize acetaldehyde to CO_2 and H_2O with a high turn-over number under visible light (>410 nm).

In the present paper, the enhanced photocatalytic activity of visible-irradiated $TiO_{2-x}N_x$ modified with co-catalysts is reported. First of all, enhancement of the rates of photooxidation of acetaldehyde by loading of Fe ions onto $TiO_{2-x}N_x$ is investigated as another choice of co-catalyst. Second, the rates of photooxidation of formic acid, acetic acid, acetaldehyde and toluene over $TiO_{2-x}N_x$s loaded with Fe, Cu or nanoscaled Pt are also compared. The difference in the degradation mechanism depending on the loaded species is also discussed.

2. Experimental

The bare $TiO_{2-x}N_x$ powder samples were prepared by treating anatase TiO_2 powder (ST01. Ishihara Sangyo Kaisha, Osaka, Japan) in an NH_3 flow at 600 °C for 3 h, followed by annealing at 300 °C for 2 h in air [6,27]. The concentration of nitrogen was found to be ~0.25 at.% with X-ray photoelectron spectroscopy (XPS). Loading was performed by impregnation of $TiO_{2-x}N_x$ with aqueous solutions of $Fe(NO_3)_3$, $Cu(NO_3)_2$ (Wako Pure Chemical Industries Ltd., Osaka, Japan), and Pt nitrate (Tanaka Kikinzoku Kogyo K. K., Tokyo, Japan) at room temperature, followed by stirring for 1 h and heating at 150 °C for water evaporation. Finally, the catalysts were calcined at 300 °C for 2 h in the cases of Fe and Cu, and at 400 °C in the case of Pt. The optimum temperatures were carefully chosen from postannealing conditions between 150 and 500 °C. The amount of loaded species was 0.5 wt.% for both Fe and Pt. Prior to the present experiment, it was confirmed that 0.5–0.8 and 0.5 wt.% gave the highest photocatalytic reaction rates under visible light for the loading of Fe and Pt, respectively. These values were selected through a similar process to that used for Cu loading [27]. Photoreductive loading of these metallic species using a high pressure mercury lamp was also performed. As a result, it was found that the photoreductive process is less effective for enhancing the rate of photooxidation of present $TiO_{2-x}N_x$.

X-ray photoelectron spectroscopy (XPS) and X-ray induced Auger electron spectroscopy (XAES) analyses were performed with a VG Microtech MT500, which was operated with Mg Kα radiation as the excitation source. The binding energies of all peaks were referenced to the Ti 2p line (458.8 eV) for TiO_2 and checked against the C 1s line (284.6 eV) originating from surface impurity carbons. Diffuse reflectance spectra in the wavelength range from 350 to 700 nm were obtained using a Varian DMS 90 spectrophotometer equipped with a reflectance sphere. Transmission electron micrographs were obtained with a JEOL JEM-200 CX TEM using an acceleration voltage of 200 kV.

The photocatalytic activities were investigated as the decomposition of gaseous acetaldehyde under visible light irradiation. The photoreactivity experiments were carried out in a Pyrex-glass vessel with a volume of 1.0 L, containing 100 ± 0.5 mg of a catalyst uniformly spread over the irradiation area. The photocatalytic reactor was purged with dry O_2 (20%)/N_2 gas and then sealed with a rubber septum [27]. Then, 3% of gaseous acetaldehyde balanced with N_2 (Takachiho Chemical Industrial Co., Ltd., Tokyo, Japan) was injected into it so that the nominal acetaldehyde concentration was about 1000 ppm. However, to compare the reaction rates for various gaseous compounds, they were injected up to 300 ppm. For toluene, acetic acid, and formic acid, one of them (high quality grade. Wako Pure Chemical Industries, Ltd., Osaka, Japan) was injected in liquid form using a microsyringe up to a nominal concentration of 300 ppm. Before irradiation, the reaction vessel was kept in the dark for 14 h. We confirmed that the concentration of the reactant in the vessel reached a constant level, indicating an adsorption equilibrium was attained. To determine the constituents of the gas phase in the reactor, gas concentrations were measured by gas chromatography. Visible light was obtained with a white fluorescent lamp (Toshiba Corporation, Tokyo, Japan) covered with an optical high-pass (>410 nm) filter (SC42, Fuji Photo Film Co., Ltd., Tokyo, Japan). The light power was approximately 0.9 mW/cm^2 (UD40 detector, TOPCON Corporation, Tokyo, Japan) at the position of the catalyst. The temperature was 26° and 35 ± 3° in the dark and in the case of irradiation, respectively. The measurement of catalytic oxidation of the samples was performed three times or more for each set of experimental condition. Surface analysis of the powders after the GC measurement was performed with DRIFT (Nicolet 6700, Thermo Electron Corporation, Madison, WI) with a TGS detector. The corresponding accessory and experimental conditions were given in a previous paper [15].

3. Results and discussion

The X-ray diffraction patterns of $TiO_{2-x}N_x$ photocatalysts were all assigned to the anatase polycrystalline phase, and no peaks for the rutile and brookite phases were detected. The average crystalline sizes of the photocatalysts were determined

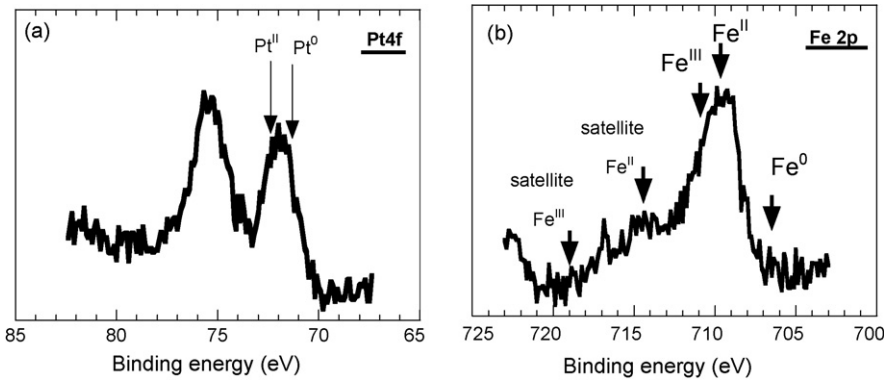

Fig. 1. XPS spectra of 0.5 wt% Pt–$TiO_{2-x}N_x$ (a) and 0.5 wt.% Fe–$TiO_{2-x}N_x$ (b).

according to Scherrer's equation using the full-width at half-maximum (FWHM) of each peak. The average crystallite sizes were estimated to be ~20 nm. In the XRD patterns of Fe, Cu or Pt loaded $TiO_{2-x}N_x$, diffraction peaks derived from the loaded particles were not detected. In a TEM photograph of the sample loaded with 0.5 wt.%-Pt, nanoscale Pt particles (1–2 nm in size) were clearly observed on the surface of the $TiO_{2-x}N_x$. On the contrary, particles were not observed on the Fe and Cu loaded samples, which was presumably due to their small particle sizes [28].

In order to investigate the chemical states of Pt and Fe, XPS measurements were performed. Fig. 1(a) shows the XPS spectrum of 0.5 wt.% Pt loaded $TiO_{2-x}N_x$. The binding energies of the Pt 4f band were 71.9 and 75.4 eV, respectively, suggesting that nanoscale Pt of 1–2 nm in size comprised a mixture of metallic Pt (71.2 eV [23]) and PtO (72.4 eV [23]) on the catalyst surface. It is speculated that the positive shift of 0.7 eV from the metallic Pt(0) state is due to superpositioning of the chemical states of the surface and the bulk of metallic Pt, and the interface between Pt and $TiO_{2-x}N_x$, because the size of Pt is less than the depth of the X-ray photoemission. The spectra for Cu were identical to those reported in a previous paper [27].

Fig. 1(b) shows the XPS spectrum of 0.5 wt% Fe loaded $TiO_{2-x}N_x$. The binding energy of the Fe 2p band was 709.5 eV, suggesting that FeO or Fe^{2+} hydroxides was present on the catalyst surface. The peak at 710.9 eV corresponding to Fe^{3+} was small (less than the XPS resolution of 0.05 at.%). In this experiment, it can be speculated that Fe^{2+} was detected due to photocatalytic reduction from Fe^{3+} to Fe^{2+} by conduction-band electron of $TiO_{2-x}N_x$ during the XPS measurement in vacuum (without any hole scavenger). However, we consider that this is negligible because reduced Ti^{3+} (from Ti^{4+} to Ti^{3+}) was not detected in the case of bare $TiO_{2-x}N_x$.

The optical absorption spectra for TiO_2, bare $TiO_{2-x}N_x$, Pt–$TiO_{2-x}N_x$ and Fe–$TiO_{2-x}N_x$ obtained by the diffuse reflection method are shown in Fig. 2. A noticeable shift in the absorption edge into the visible light region up to 550 nm was observed for bare $TiO_{2-x}N_x$ whose color was yellow, as reported previously [6,7]. The spectra of bare $TiO_{2-x}N_x$ and Pt–$TiO_{2-x}N_x$ exhibited similar absorbance in the wavelength region shorter than 400 nm. However, Pt–$TiO_{2-x}N_x$ absorbed more photons between 400 and 670 nm, resulting in a light brown color. Fe–$TiO_{2-x}N_x$ also absorbed more photons than bare $TiO_{2-x}N_x$ in the visible region up to 670 nm, resulting in a light brown color.

Fig. 3(a) and (b) illustrates the photocatalytic activities of TiO_2 (ST01), bare $TiO_{2-x}N_x$, and Fe–$TiO_{2-x}N_x$ under visible light. They show changes in the acetaldehyde and CO_2 concentrations in the gas phase of the vessel, respectively, as a function of the irradiation time. In this experiment, 1000 and 1200 ppm acetaldehyde were injected onto unloaded/loaded $TiO_{2-x}N_x$s and TiO_2, respectively. In Fig. 3(a), the scattering in the initial concentration of acetaldehyde is attributable to the adsorption characteristics of each sample. In other words, TiO_2 (ST01) adsorbs more acetaldehyde than bare $TiO_{2-x}N_x$ or Fe–$TiO_{2-x}N_x$ does, while Fe loading did not improve the adsorption of acetaldehyde. From Fig. 3(a), it was found that Fe loading onto $TiO_{2-x}N_x$ markedly enhanced the rate of acetaldehyde photodegradation. Upon irradiation with visible light, the gaseous acetaldehyde concentration dramatically decreased in the case of Fe–$TiO_{2-x}N_x$. It took only 2.3 h for complete depletion of acetaldehyde in the gas phase, whereas 4 ppm acetaldehyde was still detected after 5.5 h irradiation for bare $TiO_{2-x}N_x$, as shown in Fig. 3(a). It is worth mentioning

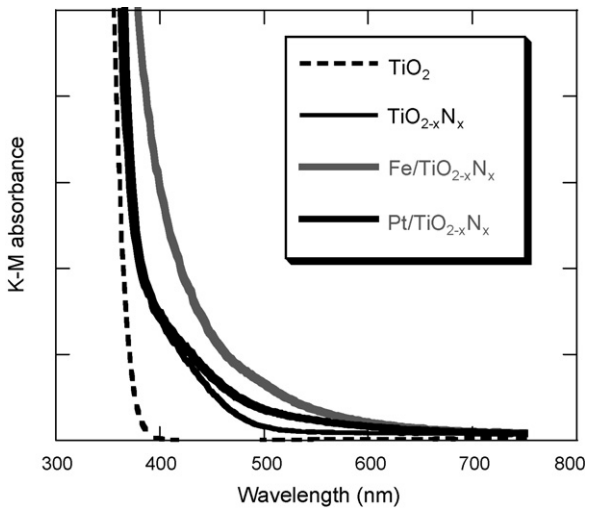

Fig. 2. The optical absorption spectra of TiO_2, bare $TiO_{2-x}N_x$, Fe–$TiO_{2-x}N_x$ and Pt–$TiO_{2-x}N_x$ obtained by the diffuse reflection method.

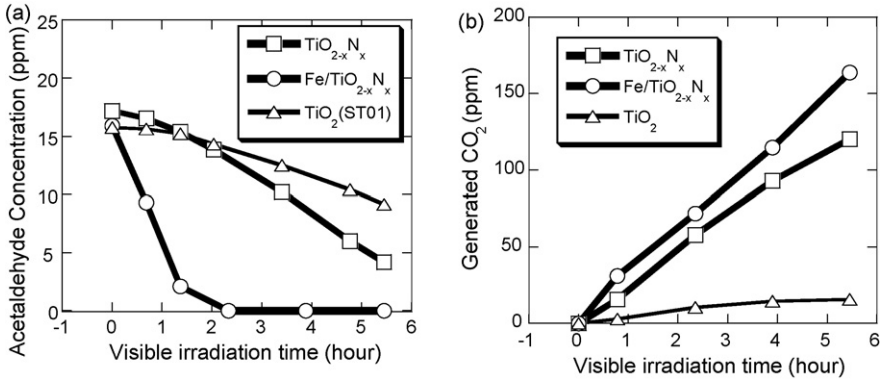

Fig. 3. Acetaldehyde (a) and CO_2 (b) concentration in the gas phase of the vessel as a function of the visible light irradiation time. These results exhibit the photocatalytic activities of TiO_2, bare $TiO_{2-x}N_x$ and Fe–$TiO_{2-x}N_x$ under visible light.

that a much longer time is required for complete photooxidation of acetaldehyde, because 2000 ppm CO_2 evolution from 1000 ppm acetaldehyde was not attained after 5.5 h irradiation, as shown in Fig. 3(b). This implies that a large number of intermediate species remained on the photocatalyst surface, suggesting that the oxidation of acetic acid, formaldehyde, and/or formic acid would be the rate-limiting step of the photooxidation of acetaldehyde in the $TiO_{2-x}N_x$ system under visible illumination. Over TiO_2, CO_2 evolution was scarcely observed, as shown in Fig. 3(b), indicating that acetaldehyde was hardly photooxidized to CO_2 over TiO_2 under visible light. This is consistent with the results of the previous GC–MS study which demonstrated that CO_2 was not produced in the effluent of the gaseous acetaldehyde flow over TiO_2 under visible light irradiation, only acetic acid being detected [16]. It was roughly estimated that 75 μmol of carbon remained on the surface of Fe–$TiO_{2-x}N_x$ after 5.5 h irradiation (corresponding to 2.2 mg acetic acid on the surface of 100 mg catalyst, assuming that carbon atoms that had not been oxidized to CO_2 remained in the form of acetic acid). For bare $TiO_{2-x}N_x$ and TiO_2, the amounts of residual carbon species on the catalyst surfaces were estimated to be 2.3 and 2.6 mg of acetic acid, respectively. These results suggest that the surfaces of these catalysts were covered by a large amount of intermediate species at this stage.

As for the long-term stability of Fe–$TiO_{2-x}N_x$, it was proved that more than 2300 μmol of CO_2 was produced when acetaldehyde had been continuously photooxidized for 110 consecutive days over 1100 μmol of Fe–$TiO_{2-x}N_x$ under visible light irradiation. This would correspond to an exposure time of 6.7 consecutive years at 150 lx assuming a linear dependence of the CO_2 generation rate on the illuminance (or number of photons) between 0.9 mW/cm^2 and 44 μW/cm^2 (at 150 lx). After this long-term stability test, the CO_2 generation rates for bare $TiO_{2-x}N_x$ and Fe-loaded $TiO_{2-x}N_x$ were found to have decreased to 51 and 70%, respectively. This suggests that loading of Fe not only enhanced the photooxidation rate, but also played a rather positive role in preventing deactivation of $TiO_{2-x}N_x$ in the long term.

Fig. 4 exhibits the time dependence of the concentration of CO_2 generated from formic acid over Pt–$TiO_{2-x}N_x$. Fig. 4(a) shows the oxidative formation of CO_2 in the absence of light. Only in this experiment, the measurement of the CO_2 concentration was started immediately after the gas injection because it was found that acetic acid was oxidized to CO_2 over Pt–$TiO_{2-x}N_x$ in the dark. On the contrary, no CO_2 was produced on bare or Fe–$TiO_{2-x}N_x$ in the dark. It is well-known that nanoscale noble metals supported on oxides exhibit a catalytic reaction without light irradiation at ambient atmospheric temperature. Burch et al. reported that the loading of nanoscale Pt [29,30] onto TiO_2 gave high activities for CO and propane oxidation without irradiation at around 20 °C. Einaga et al. reported that Pt/TiO_2 was active as to the oxidation of CO to

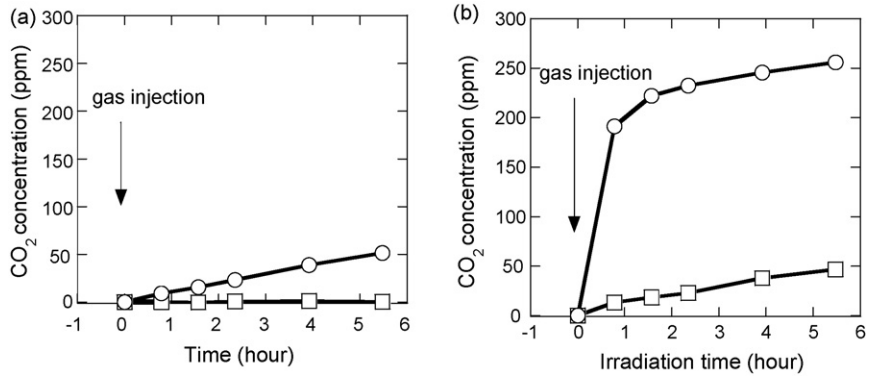

Fig. 4. CO_2 generation from formic acid over bare $TiO_{2-x}N_x$ and Pt–$TiO_{2-x}N_x$ at room temperature (26°). Thermal catalysis in the dark (a) and photocatalysis under visible light (b).

CO_2 in the dark at ambient temperature, while pure TiO_2 was not. They stated that an ESR study proved that O^- and O_3^- stabilized on Pt/TiO_2 were responsible for the reaction [31]. Miachon et al. reported that formic acid was decomposed in a membrane reactor with 0.27% Pt (4–5 nm) on TiO_2 [32]. A similar mechanism could be applicable to the present $TiO_{2-x}N_x$ loaded with Pt (1–2 nm in size). As for the oxidation of larger molecules adsorbed on Pt–$TiO_{2-x}N_x$, it was found that acetic acid, acetaldehyde and toluene could not be oxidized to CO_2 in the dark.

Fig. 4(b) shows the formation of CO_2 under visible light irradiation (>410 nm, 0.9 mW/cm^2). Over irradiated bare $TiO_{2-x}N_x$, it was obvious that CO_2 was produced from formic acid. Mrowetz et al. drew attention to the fact that the holes generated on N-doped TiO_2 by visible photons were unable to oxidize HCOO- in aqueous media. On the contrary, this result clarified that formic acid was decomposed to CO_2 over $TiO_{2-x}N_x$ in ambient air under visible light only, dismissing the fear of Mrowetz's. This suggests that adsorbed gaseous O_2 and conduction band electrons play important roles in photocatalytic oxidation over N-doped TiO_2 with a hybridized or isolated impurity level of N just above the valence band maximum [7,12]. The adsorbed O_2s and the photogenerated electrons can form superoxide radical anions and singlet oxygens through triplet–triplet energy transfer [8], presumably followed by the formation of hydrogen peroxide or other radical species such as $^{\bullet}OH$ [33,34]. However, at present, the rate of generation of CO_2 from formic acid over visible-irradiated $TiO_{2-x}N_x$ is as low as that for non-irradiated Pt loaded $TiO_{2-x}N_x$.

The rates of generation of CO_2 from formic acid over Fe, Cu and Pt-loaded $TiO_{2-x}N_x$ are shown in Table 1. These rates were calculated from the CO_2 concentrations generated after 5.5 h reaction. Only in the case of formic acid over irradiated Pt–$TiO_{2-x}N_x$, the rate was determined from the value after 1.3 h irradiation to avoid underestimation due to CO_2 saturation. The rate over bare $TiO_{2-x}N_x$ was found to be 11 times higher than that for TiO_2. Intriguingly, on Pt loading, the rate of CO_2 generation over $TiO_{2-x}N_x$ was enhanced 22 times. This is probably due to a combined effect of the thermal catalysis of nanoscale Pt that occurs even in the dark and the photocatalysis of Pt–$TiO_{2-x}N_x$. The rates were also enhanced by factors of 5.2 and 6.3 by Fe and Cu loading, respectively, though these photocatalysts exhibit no oxidative power in the dark.

Table 1
The rates of CO_2 generation from formic acid, acetic acid, acetaldehyde and toluene over TiO_2 (ST01), bare $TiO_{2-x}N_x$, Fe–$TiO_{2-x}N_x$, Cu-$TiO_{2-x}N_x$, and Pt–$TiO_{2-x}N_x$ under visible light irradiation (>410 nm). The rates of CO_2 generation from formic acid in the dark are also indicated

Organic substance	Rate of CO_2 generation under visible light (>410 nm) (ppm/h)				
	$TiO_{2-x}N_x$	$Pt/TiO_{2-x}N_x$	$Fe/TiO_{2-x}N_x$	$Cu/TiO_{2-x}N_x$	TiO_2
HCOOH (darkness)	0.0	16.7	0.0	0.0	0.0
HCOOH	5.5	123.6	28.5	34.6	0.5
CH3COOH (darkness)	0.0	0.0	0.0	0.0	0.0
CH_3COOH	6.0	15.0	12.4	25.0	2.7
CH_3CHO	20.1	30.6	32.7	33.1	3.6
C_7H_8	9.8	14.5	10.4	9.9	0.5

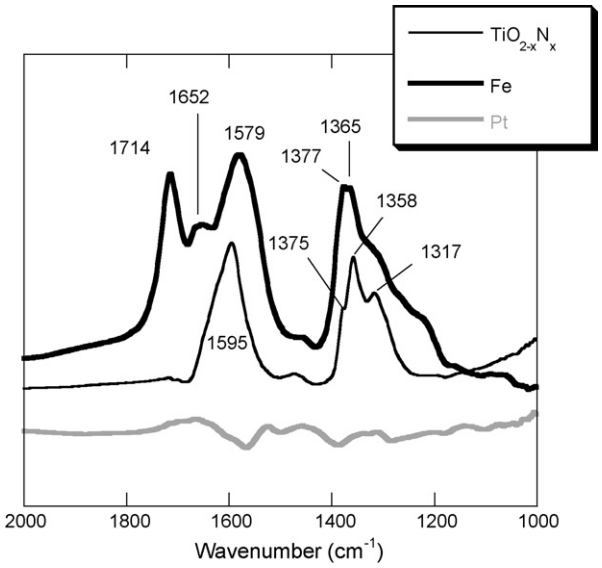

Fig. 5. DRIFT spectra of bare $TiO_{2-x}N_x$, Fe–$TiO_{2-x}N_x$, and Pt–$TiO_{2-x}N_x$ samples used for formic acid photodegradation. These spectra are obtained after 5.5 h decomposition under visible light irradiation followed by a subsequent 14 h storage in the dark.

To investigate intermediate species on the catalyst surfaces, DRIFT spectra of bare, Fe–$TiO_{2-x}N_x$, and Pt–$TiO_{2-x}N_x$ are shown in Fig. 5. They were measured after 5.5 h degradation of formic acid under visible irradiation followed by subsequent 14 h storage in the dark. No signals originating from the vibrational or stretching mode of formate adsorbed were observed on the surface of Pt–$TiO_{2-x}N_x$, indicating that residual formic acid (44 ppm of formic acid remained in the gas-phase in the reaction vessel after 5.5 h visible irradiation) had been completely oxidized to CO_2 during 14 h exposure to the air. On the contrary, strong peaks of formic acid and formate were detected for bare and Fe–$TiO_{2-x}N_x$. The peaks between 1660–1570 and 1380–1310 cm^{-1} are assignable to asymmetric $\nu_{as(HCOO-)}$ and symmetric $\nu_{s(HCOO-)}$ formate characteristic vibrations, respectively, which was speculated based on the previous reports on TiO_2 and Fe-doped TiO_2 [35,36]. In addition to formate bands, other $\nu_{C=O}$ (1714 cm^{-1}) and ν_{CO-OH} (1206–1200 cm^{-1}) vibration bands, which appear at slightly different wavenumbers to those in the case of free formic acid (1730 and 1200 cm^{-1}, respectively) [35,36] were observed only on Fe–$TiO_{2-x}N_x$. This shows that the adsorption in the CO–OH form on the Fe site might also be a cause of the enhanced photooxidation under visible light.

Table 1 also summarizes the rates of CO_2 generation from acetic acid, acetaldehyde, and toluene over various photocatalysts irradiated with visible light. It was confirmed that the rate for acetaldehyde over bare $TiO_{2-x}N_x$ was about 6 times higher than that over TiO_2, as described in a previous paper [7]. On the contrary, the effect of N-doping on acetic acid oxidation was low compared to that on acetaldehyde oxidation because it was only 2.2 times higher than that for TiO_2. However, Fe, Cu and Pt loading improved the rate of acetic acid oxidation over

bare $TiO_{2-x}N_x$. Among them, Cu loading causes a significant improvement in acetic acid oxidation, showing a higher rate enhancement by a factor of 4.2.

Muggli et al. reported the reaction pathway for ethanol in which *alpha*-carbon was labeled with ^{13}C over TiO_2 [37]. They found that ethanol was decomposed into acetaldehyde ($CH_3{}^{13}CHO$) first of all, and that its *alpha*-carbon was preferentially oxidized to CO_2 as the two carbon species was sequentially oxidized. Thus, they concluded that there are at least two parallel pathways from acetaldehyde to CO_2 and H_2O, only one of which involves acetic acid. In this case, it is plausible that the improved rate for acetic acid on loading of Cu is due to the change in the degradation pathway caused by surface Cu species. In DRIFT spectra obtained during acetaldehyde or toluene degradation over bare, Fe, Cu and Pt loaded photocatalysts, Cu showed a different proportion of surface intermediate species. This also might be correlated with the characteristic feature of the Cu–$TiO_{2-x}N_x$.

As for toluene photooxidation, the CO_2 generation rate was improved only in the case of Pt-loading. In the process of photodegradation of toluene over $TiO_{2-x}N_x$ revealed by *in situ* DRIFT [15], the side-chain methyl (–CH_3) was initially oxidized to yield mainly benzaldehyde and benzylalcohol, resulting in strong adsorption on the photocatalyst surface, followed by ring-opening to produce carboxylic acids. On the surfaces of Fe, Cu and Pt loaded $TiO_{2-x}N_x$, these very fast initial processes were observed by *in situ* DRIFTs. Therefore, it is speculated that Fe and Cu loading is not effective for promoting the ring-opening of aromatics such as benzaldehyde and benzylalcohol over a $TiO_{2-x}N_x$ like Pt–$TiO_{2-x}N_x$.

For the $TiO_{2-x}N_x$ system, it has been reported that only Cu and Pt loading enhanced the rate of acetaldehyde photooxidation, while Ni, Zn and La did not [27]. For the present system, it is worth noting that the loading of Fe also enhanced the rates of photooxidation of acetaldehyde and other organic compounds like Cu. However, in the dark, Fe and Cu were not effective as to formic acid oxidation to CO_2, which is different from the case of Pt. Therefore, some different mechanisms might be possible for the improved rates over Fe and Cu loaded $TiO_{2-x}N_x$. Before irradiation (for example, in Fig. 3(a)), the residual concentrations of gaseous species over loaded $TiO_{2-x}N_x$ were nearly equal to or higher than that for bare $TiO_{2-x}N_x$ after 14 h storage in the dark. Judging from this fact, the difference in the gas adsorption is not the main cause of the enhanced photoactivity. The ESR experiment for Fe–$TiO_{2-x}N_x$ shown in Fig. 6 proved that the Fe^{3+} (less than 0.05 at.% with XPS) signal was very small and intriguingly did not respond to visible light irradiation. In this experiment, it was confirmed that reduction of Fe^{3+} to Fe^{2+} by photoelectrons produced in $TiO_{2-x}N_x$ was negligible because the catalysts were set in a light shielded box. This suggests that Fe^{2+} (>0.5 at.%) remained stable on the catalyst surface so that the ratio Fe^{3+}/Fe^{2+} was independent of photoirradiation. This suggests that Fe^{2+} was originally stable on the surface of $TiO_{2-x}N_x$ in the dark. Interestingly, these results are different from those reported by Ohno et al. who found photoresponsive Fe^{3+} ions were detected with XPS on the surface of cationic S-doped TiO_2 [38].

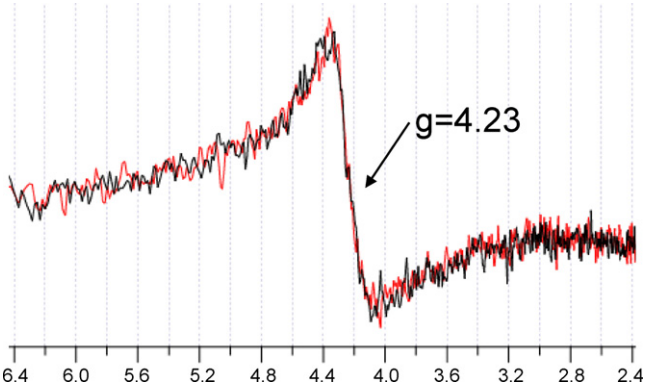

Fig. 6. ESR spectra of Fe^{3+} in Fe-loaded $TiO_{2-x}N_x$ measured at 20 K. The signals were obtained both in the dark (black line) and under visible irradiation (>410 nm, red line). (For interpretation of the references to color in this figure legend, the reader is referred to the web version of the article.)

Therefore, for the present system, we propose that an increase in the amount of produced $^{\bullet}OH$ due to a Fenton type process could be possible throughout the irradiation. Fenton process generally involves the application of iron salts and hydrogen peroxide to produce hydroxyl radicals, Eqs. (1) and (2) [39–42]:

$$Fe^{2+} + H_2O_2 \rightarrow Fe^{3+} + OH^- + {}^{\bullet}OH \quad (1)$$

$$Fe^{3+} + H_2O_2 \rightarrow Fe^{2+} + HO_2{}^{\bullet} + H^+ \quad (2)$$

In the present case, Fe^{3+} in Eq. (2) can also be recovered immediately to Fe^{2+} by photogenerated conduction-band electrons of $TiO_{2-x}N_x$. The same Fenton-like reaction can take place on Cu^{1+} loaded $TiO_{2-x}N_x$.

As seen on comparison of these three photocatalysts loaded with metallic species, they have their own advantages. From the viewpoint of cost, Fe^{2+} or Cu^{1+} loading onto $TiO_{2-x}N_x$ is preferable. Cu^{1+} is more preferable in view of antibacterial properties [27] and acetic acid decomposition, while Fe^{2+} is preferable for long-term stability. However, nanoscale Pt loading is advantageous for the degradation of a wide variety of gaseous species. Since formic acid is formed from almost all the organic gaseous species during the process of oxidation to CO_2 and H_2O, thermal catalysis by Pt–$TiO_{2-x}N_x$ at ambient temperature is also attractive when it is used under weak interior lighting. Consequently, a nanosize Au catalyst active at ambient temperature [43,44] as well as Pt may be applicable to the present system. The combination of co-loading of nanoscale metals exhibiting thermal catalysis at ambient temperature and Fe^{2+} and/or Cu^{1+} onto $TiO_{2-x}N_x$ might be the best choice for indoor applications.

4. Conclusions

Nitrogen-doped TiO_2 photocatalysts loaded with Fe^{2+} or Cu^{1+} ions, or nanoscale Pt were prepared. The rates of photocatalytic oxidation by the catalysts under visible light irradiation (>410 nm) were examined for gaseous toluene, acetaldehyde, acetic acid and formic acid at room temperature. It was found that loading of Fe, Cu or Pt resulted in similar rate

enhancement of acetaldehyde oxidation, and that Cu and Pt gave the highest rates of acetic acid and toluene oxidation, respectively. It was also confirmed that the rate of formic acid photooxidation was enhanced by factors of 5 and 22 on loading of Fe and Pt, respectively. The extremely high rate of enhancement of formic acid oxidation over Pt–$TiO_{2-x}N_x$ was found to be due to a combined effect of photocatalysis and thermal catalysis at room temperature facilitated by nanoscale Pt (1–2 nm). Therefore, making use of the combined effect of oxidation of gaseous pollutants by visible photons absorbed in $TiO_{2-x}N_x$ and dark catalysis of nanoscale metallic species on the $TiO_{2-x}N_x$ is one of the practical methods for air purification under interior lighting, etc.

Acknowledgments

The authors thank N. Takahashi, K. Kitazumi and Y. Akimoto for the XPS and TEM analyses, and are also grateful to M. Yamaguchi and Y. Taga for their support.

References

[1] M.A. Fox, M.T. Dulay, Chem. Rev. 93 (1993) 341.
[2] O. Legrini, E. Oliveros, A.M. Braun, Chem. Rev. 93 (1993) 671.
[3] D.F. Ollis, H. Al-Ekabi, Photocatalytic Purification and Treatment of Water and Air, Elsevier, Amsterdam, 1993.
[4] M.R. Hoffmann, S.T. Martin, W. Choi, D.W. Bahnemann, Chem. Rev. 95 (1995) 69.
[5] S. Sato, Chem. Phys. Lett. 123 (1986) 126.
[6] T. Morikawa, R. Asahi, T. Ohwaki, K. Aoki, Y. Taga, Jpn. J. Appl. Phys. 40 (2001) L561.
[7] R. Asahi, T. Morikawa, T. Ohwaki, K. Aoki, Y. Taga, Science 293 (2001) 269.
[8] C. Lettmann, K. Hildenbrand, H. Kisch, W. Macyk, W.F. Maier, Appl. Catal. B 32 (2001) 215.
[9] T. Umebayashi, T. Yamaki, H. Itoh, K. Asai, Appl. Phys. Lett. 81 (2002) 454.
[10] T. Ohno, T. Mistui, M. Matsumura, Chem. Lett. 32 (2003) 364.
[11] K. Aoki, T. Morikawa, T. Ohwaki, Y. Taga, in: D.E. Ollis, H. Al-Ekabi (Eds.), Photocatalytic and Advanced Oxidation Processes for the Treatment of Air, Water, Soil and Surfaces, Redox Technologies Inc., Ontario, Canada, 2005, p. 59.
[12] T. Tachikawa, Y. Takai, S. Tojo, M. Fujitsuka, H. Irie, K. Hashimoto, T. Majima, J. Phys. Chem. B 110 (2006) 13158.
[13] R. Nakamura, T. Tanaka, Y. Nakato, J. Phys. Chem. B 108 (2004) 10617.
[14] M. Mrowetz, W. Balcerski, A.J. Colussi, M.R. Hoffmann, J. Phys. Chem. B 108 (2004) 17269.
[15] Y. Irokawa, T. Morikawa, K. Aoki, S. Kosaka, T. Ohwaki, Y. Taga, Phys. Chem. Chem. Phys. 8 (2006) 1116.
[16] American Ceramic Society Bulletin, vol. 85, 2006, p. 23.
[17] K. Aoki, T. Morikawa, T. Ohwaki, Y. Taga, Chem. Lett. 35 (2006) 616.
[18] S. Sato, J.M. White, Chem. Phys. Lett. 72 (1980) 83.
[19] H. Einaga, S. Futamura, T. Ibusuki, Environ. Sci. Technol. 35 (2001) 1880.
[20] G. Colon, M. Maicu, M.C. Hidalgo, J.A. Navıo, Appl. Catal. B 67 (2006) 41.
[21] J.M. Herrmann, J. Disdier, P. Pichat, Chem. Phys. Lett. 108 (1984) 618.
[22] S. Ikeda, N. Sugiyama, B. Pal, G. Marcí, L. Palmisano, H. Noguchi, K. Uosaki, B. Ohtani, Phys. Chem. Chem. Phys. 3 (2001) 267.
[23] J. Lee, W. Choi, J. Phys. Chem. B 109 (2005) 7399.
[24] A. Linsebigler, C. Rusu, J.T. Yates Jr., J. Am. Chem. Soc. 118 (1996) 5284.
[25] B. Ohtani, R.M. Bowman, D.P. Colombo, H. Kominami, H. Noguchi, K. Uosaki, Chem. Lett. 7 (1998) 579.
[26] A. Furube, T. Asahi, H. Masuhara, H. Yamashita, M. Anpo, Chem. Phys. Lett. 336 (2001) 424.
[27] T. Morikawa, Y. Irokawa, T. Ohwaki, Appl. Catal. A 314 (2006) 123.
[28] Y. Nagai, T. Hirabayashi, K. Dohmae, N. Takagi, T. Minami, H. Shinjoh, S. Matsumoto, J. Catal. 242 (2006) 103.
[29] R. Burch, M.J. Hayes, D.J. Crittle, Catal. Today 47 (1999) 229.
[30] K. Rutha, M. Hayes, R. Burch, S. Tsubota, M. Haruta, Appl. Catal. B 24 (2000) L133.
[31] H. Einaga, A. Ogata, S. Futamura, T. Ibusuki, Chem. Phys. Lett. 338 (2001) 303.
[32] S. Miachon, V. Perez, G. Crehan, E. Torp, H. Ræder, R. Bredesen, J.A. Dalmon, Catal. Today 82 (2003) 75.
[33] W. Kubo, T. Tatsuma, Anal. Sci. 20 (2004) 591.
[34] R. Nakamura, A. Imanishi, K. Murakoshi, Y. Nakato, J. Am. Chem. Soc. 125 (2003) 7443.
[35] J. Araña, O.G. Díaz, M.M. Saracho, J.M.D. Rodŕıguez, J.A.H. Melián, J.P. Peña, Appl. Catal. B 32 (2001) 49.
[36] L.F. Liao, W.C. Wu, C.Y. Chen, J.L. Lin, J. Phys. Chem. B 105 (2001) 7678.
[37] D.S. Muggli, J.T. McCue, J.L. Falconer, J. Catal. 173 (1998) 470.
[38] T. Ohno, Z. Miyamoto, K. Nishijima, H. Kanemitsu, F. Xueyuan, Appl. Catal. A 302 (2006) 62.
[39] M.A. Tarr, in: M.A. Tarr (Ed.), Chemical Degradation Methods for Wastes and Pollutants, Marcel Decker, Inc., New York, 2003, pp. 165–201.
[40] A. Sclafani, L. Palmisano, E. Davi, J. Photochem. Photobiol. A 56 (1991) 113.
[41] H. Fallmann, T. Krutzler, R. Bauer, S. Malato, J. Blanco, Catal. Today 54 (1999) 309.
[42] C. Fox, S. Ammar, C. Arias, E. Brillas, A.V. Vargas-Zavala, R. Abdelhedi, Appl. Catal. B 67 (2006) 93.
[43] M. Haruta, N. Yamada, T. Kobayashi, S. Ijima, J. Catal. 115 (1989) 301.
[44] M. Valden, X. Lai, D.W. Goodman, Science 281 (1998) 1647.